

Recent advances and perspectives of zinc metal-free anodes for zinc ion batteries

Jiabing Miao, Yingxiao Du, Ruotong Li, Zekun Zhang, Ningning Zhao, Lei Dai, Ling Wang, and Zhangxing He

Cite this article as:

Jiabing Miao, Yingxiao Du, Ruotong Li, Zekun Zhang, Ningning Zhao, Lei Dai, Ling Wang, and Zhangxing He, Recent advances and perspectives of zinc metal-free anodes for zinc ion batteries, *Int. J. Miner. Metall. Mater.*, 31(2024), No. 1, pp. 33-47. <https://doi.org/10.1007/s12613-023-2665-y>

View the article online at [SpringerLink](#) or [IJMMM Webpage](#).

Articles you may be interested in

Zhi-yuan Feng, Wen-jie Peng, Zhi-xing Wang, Hua-jun Guo, Xin-hai Li, Guo-chun Yan, and Jie-xi Wang, [Review of silicon-based alloys for lithium-ion battery anodes](#), *Int. J. Miner. Metall. Mater.*, 28(2021), No. 10, pp. 1549-1564. <https://doi.org/10.1007/s12613-021-2335-x>

Xing-hua Qin, Ye-hong Du, Peng-chao Zhang, Xin-yu Wang, Qiong-qiong Lu, Ai-kai Yang, and Jun-cai Sun, [Layered barium vanadate nanobelts for high-performance aqueous zinc-ion batteries](#), *Int. J. Miner. Metall. Mater.*, 28(2021), No. 10, pp. 1684-1692. <https://doi.org/10.1007/s12613-021-2312-4>

Dan Wang, Qun Ma, Kang-hui Tian, Chan-Qin Duan, Zhi-yuan Wang, and Yan-guo Liu, [Ultrafine nano-scale Cu₂Sb alloy confined in three-dimensional porous carbon as an anode for sodium-ion and potassium-ion batteries](#), *Int. J. Miner. Metall. Mater.*, 28(2021), No. 10, pp. 1666-1674. <https://doi.org/10.1007/s12613-021-2286-2>

Qi Wang, Yue-yong Du, Yan-qing Lai, Fang-yang Liu, Liang-xing Jiang, and Ming Jia, [Three-dimensional antimony sulfide anode with carbon nanotube interphase modified for lithium-ion batteries](#), *Int. J. Miner. Metall. Mater.*, 28(2021), No. 10, pp. 1629-1635. <https://doi.org/10.1007/s12613-021-2249-7>

Li-fen Guo, Shi-yun Zhang, Jian Xie, Dong Zheng, Yuan Jin, Kang-yan Wang, Da-gao Zhuang, Wen-quan Zheng, and Xin-bing Zhao, [Controlled synthesis of nanosized Si by magnesiothermic reduction from diatomite as anode material for Li-ion batteries](#), *Int. J. Miner. Metall. Mater.*, 27(2020), No. 4, pp. 515-525. <https://doi.org/10.1007/s12613-019-1900-z>

Ying-jun Qiao, Huan Zhang, Yu-xin Hu, Wan-peng Li, Wen-jing Liu, Hui-ming Shang, Mei-zhen Qu, Gong-chang Peng, and Zheng-wei Xie, [A chain-like compound of Si@CNT nanostructures and MOF-derived porous carbon as an anode for Li-ion batteries](#), *Int. J. Miner. Metall. Mater.*, 28(2021), No. 10, pp. 1611-1620. <https://doi.org/10.1007/s12613-021-2266-6>



IJMMM WeChat



QQ author group

Recent advances and perspectives of zinc metal-free anodes for zinc ion batteries

Jiabing Miao^{1,2)}, Yingxiao Du³⁾, Ruotong Li³⁾, Zekun Zhang^{3),✉}, Ningning Zhao³⁾, Lei Dai^{3),✉}, Ling Wang³⁾, and Zhangxing He^{3),✉}

1) Science and Technology Innovation Center of Circular Economy, Ha'erwusu Open-Pit Coal Mine, China Shenhua Energy Co., Ltd., Ordos 010300, China

2) Research Center of Comprehensive Utilization of Coal Associated Resources, National Energy Group, Ordos 010300, China

3) School of Chemical Engineering, North China University of Science and Technology, Tangshan 063009, China

(Received: 11 January 2023; revised: 22 March 2023; accepted: 25 April 2023)

Abstract: Zinc-ion batteries (ZIBs) are recognized as potential energy storage devices due to their advantages of low cost, high energy density, and environmental friendliness. However, zinc anodes are subject to unavoidable zinc dendrites, passivation, corrosion, and hydrogen evolution reactions during the charging and discharging of batteries, becoming obstacles to the practical application of ZIBs. Appropriate zinc metal-free anodes provide a higher working potential than metallic zinc anodes, effectively solving the problems of zinc dendrites, hydrogen evolution, and side reactions during the operation of metallic zinc anodes. The improvement in the safety and cycle life of batteries creates conditions for further commercialization of ZIBs. Therefore, this work systematically introduces the research progress of zinc metal-free anodes in “rocking chair” ZIBs. Zinc metal-free anodes are mainly discussed in four categories: transition metal oxides, transition metal sulfides, MXene (two dimensional transition metal carbide) composites, and organic compounds, with discussions on their properties and zinc storage mechanisms. Finally, the outlook for the development of zinc metal-free anodes is proposed. This paper is expected to provide a reference for the further promotion of commercial rechargeable ZIBs.

Keywords: zinc ion batteries; anode; zinc metal-free anode; recent advances; perspectives

1. Introduction

People are increasingly aware of the urgency of developing renewable energy sources in response to the massive consumption of traditional nonrenewable energy sources and pollution problems caused by coal combustion [1–2]. The full utilization of renewable and the evolution of different types of power storage systems are also popular issues of concern. Electrochemical energy storage technology has been rapidly developing in recent years. Lithium-ion batteries have dominated the power battery market [3]. However, some inherent defects of lithium, including low safety, low power density, high cost, and raw material supply problems, have hindered its application in energy storage [4–5]. Therefore, developing batteries of non-lithium-ion systems has become critical to meet the needs of different application scenarios. Among them, the demand for replacing Li-ion batteries with zinc-ion batteries (ZIBs) continues to increase [6–7]. ZIBs hold a broad application prospect within the field of energy storage due to their low cost, high safety, high power density, and environmental friendliness [8–10].

ZIBs generally comprise three fundamental components: cathode, anode, and electrolyte. The cathode, which is connected to critical indicators, such as cost, energy density, and

discharge platform, is critical to the performance of ZIBs. Vanadium oxides [11–14], manganese oxides [15–19], and Prussian blue analogs [20–22] are the most common cathode materials for ZIBs. The electrolyte is an essential part of the battery, providing a pathway for ion exchange between the cathode and the anode [23–24]. Zinc metal is an ideal anode material for ZIBs because of its abundant reserves, environmental friendliness, low cost, and low redox potential. However, dendrite growth, hydrogen evolution, and corrosion on the surface of the zinc anode are inevitable during the charging and discharging processes, and these problems severely limit the battery performance [25–26]. Therefore, a comprehensive understanding of the challenges encountered by zinc anode and their solution strategies is important for the development of highly stable and reversible ZIBs.

Various modification strategies, such as surface modifications [27–29], structural designs [30–31], zinc alloying [32–36], and electrolyte optimization [37–38], have been implemented to improve the issues of dendrite growth, corrosion, hydrogen evolution, and byproducts on the anodes [39]. These improvements have brought the performance of the modified anodes close to the level required for commercial application. However, the low discharge depth and poor plating/stripping efficiencies of the zinc anode result in low en-

✉ Corresponding authors: Zekun Zhang E-mail: zhangzekun1020@163.com;
Zhangxing He E-mail: zxhe@ncst.edu.cn

Lei Dai E-mail: dailei_b@163.com;

ergy density in the full cell despite such improvements. “Rocking chair” ZIBs have been developed to provide a proper operating potential between their electrodes to address the aforementioned issues, almost completely avoiding dendrites and hydrogen evolution problems [40]. Considering “rocking chair” ZIBs, these batteries have a high weight energy density and a long lifetime due to their rapid electronic transport dynamics, while their theoretical capacity is lower than that of zinc anodes of undefined mechanism.

Reviews of zinc metal-free anodes in this area are still fairly restricted despite the increasing attention on “rocking chair” batteries. This paper summarizes the development of zinc-free metal anodes in ZIBs (Fig. 1). First, this paper summarizes the shortages and optimization strategies for zinc anodes in ZIBs, followed by an overview of the characteristics of zinc metal-free anodes. Then, the zinc metal-free anodes are classified (Fig. 2) and introduced. Last, the future challenges and outlook for the zinc metal-free anode are discussed.

2. Issues with anodes for ZIBs and feature of zinc metal-free anodes

The emergence of dendrites, corrosion, passivation, and

hydrogen evolution on the zinc anode interface hinders the practical application of the battery during operation [55]. Zinc ions tend to deposit in areas with high electric force intensity and gradually form zinc dendrites [56], leading to battery short-circuiting in severe cases [57]. Zinc dendrites weaken the battery structure and increase the specific surface area of the anode, resulting in the occurrence of side reactions. Electrochemical corrosion also occurs on the anode surface during the discharge process [58]. These electrochemical corrosion products can cover the active sites on the anode surface and cause electrode passivation. As an amphoteric metal, zinc can evolve into hydrogen in acidic or alkaline electrolytes to produce hydrogen, which increases the battery pressure, leading to battery expansion and rupture [59].

The capacity and lifetime of the zinc anode can be negatively affected by harmful products, such as dendrite growth, corrosion, and hydrogen evolution. Despite the progress in these areas, challenges remain in completely resolving problems with zinc anodes, especially in the area of dendrite growth. In the commercialization process, researchers focus on the volume/mass energy density of the battery, which is relevant to the pocket capability of the battery. Most reported zinc metal utilization is currently limited to less than 5% and

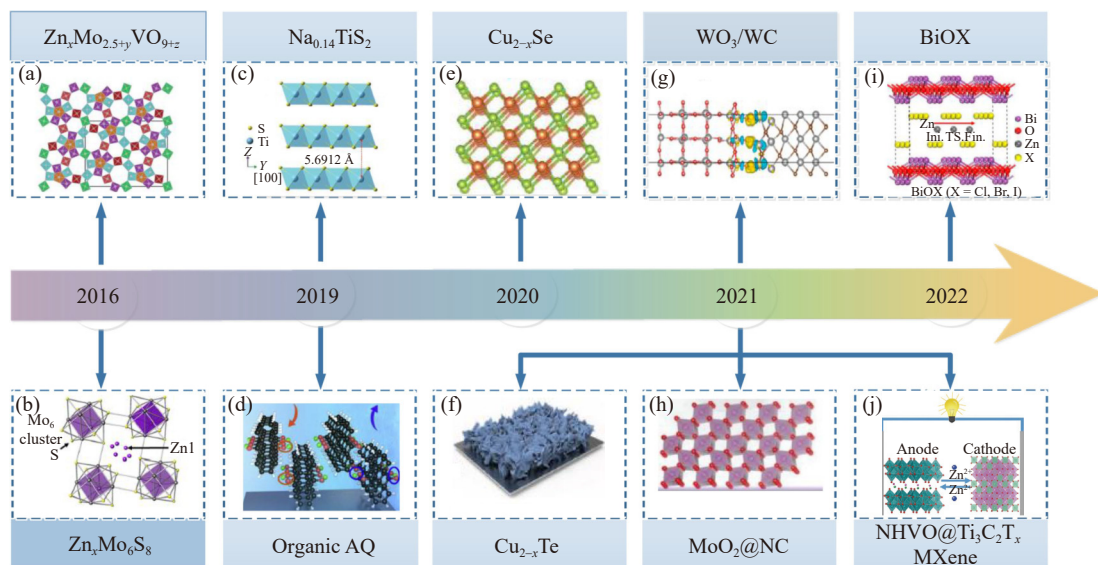


Fig. 1. Outstanding working timeline for zinc metal-free anodes in zinc ion batteries. (a) Reproduced from Ref. [41] with permission from the Royal Society of Chemistry. (b) Reprinted with permission from M.S. Chae, J.W. Heo, S.C. Lim, and S.T. Hong, *Inorg. Chem.*, vol. 55, 3294–3301 (2016) [42]. Copyright 2016 American Chemical Society. (c) W. Li, K.L. Wang, S.J. Cheng, and K. Jiang, *Adv. Energy Mater.*, vol. 9, art. No. 1900993 (2019) [43]. Copyright Wiley-VCH Verlag GmbH & Co. KGaA. Reproduced with permission. (d) Reprinted from *Mater. Today Energy*, 13, L.J. Yan, X.M. Zeng, Z.H. Li, et al., An innovation: Dendrite free quinone paired with $ZnMn_2O_4$ for zinc ion storage, 323–330, Copyright 2019, with permission from Elsevier [44]. (e) Y. Yang, J.F. Xiao, J.Y. Cai, et al., *Adv. Funct. Mater.*, vol. 31, art. No. 2005092 (2021) [45]. Copyright Wiley-VCH Verlag GmbH & Co. KGaA. Reproduced with permission. (f) W. Li, Y.S. Ma, P. Li, X.Y. Jing, K. Jiang, and D.H. Wang, *Adv. Energy Mater.*, vol. 11, art. No. 2102607 (2021) [46]. Copyright Wiley-VCH Verlag GmbH & Co. KGaA. Reproduced with permission. (g) Reprinted from *Chem. Eng. J.*, V426, J. Cao, D.D. Zhang, Y.L. Yue, et al., Strongly coupled tungsten oxide/carbide heterogeneous hybrid for ultrastable aqueous rocking-chair zinc-ion batteries, art. No. 131893, Copyright 2021, with permission from Elsevier [47]. (h) B. Wang, J.P. Yan, Y.F. Zhang, M.H. Ye, Y. Yang, and C.C. Li, *Adv. Funct. Mater.*, vol. 31, art. No. 2102827 (2021) [48]. Copyright Wiley-VCH Verlag GmbH & Co. KGaA. Reproduced with permission. (i) Reprinted with permission from Q. Zhang, T.F. Duan, M.J. Xiao, et al., *ACS Appl. Mater. Interfaces*, vol. 14, 25516–25523 (2022) [49]. Copyright 2022 American Chemical Society. (j) X. Wang, Y.M. Wang, Y.P. Jiang, et al., *Adv. Funct. Mater.*, vol. 31, art. No. 2103210 (2021) [50]. Copyright Wiley-VCH Verlag GmbH & Co. KGaA. Reproduced with permission.

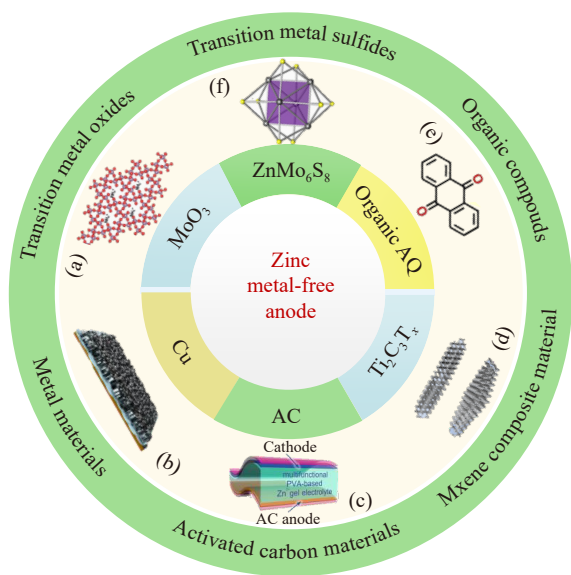


Fig. 2. Classification of zinc metal-free anode in zinc ion batteries. (a) Reproduced from Ref. [51] with permission from the Royal Society of Chemistry. (b) Reprinted with permission from Y.P. Zhu, Y. Cui, and H.N. Alshareef, *Nano Lett.*, vol. 21, 1446–1453 (2021) [52]. Copyright 2021 American Chemical Society. (c) Y.Q. Jiang, K. Ma, M.L. Sun, Y. Y. Li and J. P. Liu, *Energy Environ. Mater.*, vol. 6, art. No. e12357 (2023) [53]. Copyright Wiley-VCH Verlag GmbH & Co. KGaA. Reproduced with permission. (d) Reprinted from *Nano Energy*, 103, K. Mao, J.J. Shi, Q.X. Zhang, *et al.*, High-capacitance MXene anode based on Zn-ion pre-intercalation strategy for degradable micro Zn-ion hybrid supercapacitors, art. No. 107791, Copyright 2022, with permission from Elsevier [54]. (e) Reprinted from *Mater. Today Energy*, 13, L.J. Yan, X.M. Zeng, Z.H. Li, *et al.*, An innovation: Dendrite free quinone paired with ZnMn_2O_4 for zinc ion storage, 323–330, Copyright 2019, with permission from Elsevier [44]. (f) Reprinted with permission from M.S. Chae, J.W. Heo, S.C. Lim, and S.T. Hong, *Inorg. Chem.*, vol. 55, 3294–3301(2016) [42]. Copyright 2016 American Chemical Society.

has a low discharge depth [60]. Thus, most people fail to notice only a weak layer of zinc on the electrode surface participates in the electrochemical reaction and releases zinc ions [41–42,49].

“Rocking chair” ZIBs are developed from “rocking chair” LIBs, which markedly improved the energy density and stability of batteries [43]. The construction and mechanism of “rocking chair” ZIBs have similarities to that of “rocking chair” LIBs, with a zinc metal-free anode instead of metallic zinc. The “rocking chair” operation mechanism of ZIBs is based on the reverse flow of divalent zinc ions between the zinc metal-free anode and zinc-rich cathode. The zinc ions spread from the electrolyte and then into the anode during charging. The opposite occurs during the discharge. Zinc metal-free anode material must be stabilized and has an appropriate layer structure for normal operation.

The research of “rocking chair” ZIBs is currently expanding, especially the study of zinc-free metal anodes for “rocking chair” ZIBs. Appropriate zinc-free metal anodes provide a high working potential over metallic zinc anodes, which

can effectively inhibit zinc dendrite formations, side reactions, and hydrogen evolution, leading to enhanced security and battery cycle life. Only a few zinc-free metal anodes for “rocking chair” ZIBs have been reported due to the short-term development experience. Therefore, the capacity of most “rocking chair” ZIBs is still lower than that of conventional zinc anodes. Undoubtedly, zinc-free metal anodes for “rocking chair” ZIBs are inadequate considering energy density, failing to surpass zinc anodes. Hence, one of the largest challenges for “rocking chair” ZIBs with zinc-free metal anodes is the low capacity density. The storage mechanism of ZIBs as a multiple-valent ion battery differs from that of ordinary univalent ion batteries and requires a comprehensive study. Furthermore, studies on the electrolyte of “rocking chair” ZIBs are few, resulting in limited available types. The fundamental demands of electrolytes of “rocking chair” ZIBs include high ion electrical conductivity, wide potential window, and a well-organized eluent–electrode interface. As a new type of battery, the discovery of assembling technologies is insufficient. The selection of binders, traps, and even containers in the battery assembly process remains challenging. Consequently, “rocking chair” ZIBs have high research value as a novel kind of battery that requires considerable specific capacities, high operating voltages, and long cycle lifetimes. The investigation of the electrolyte or discovery of the battery packaging processes may potentially lead to a commercial breakthrough for “rocking chair” ZIBs.

3. Zinc metal-free anode

The use of the intercalation mechanism graphite material as the anode electrode in LIBs effectively addresses the lithium dendrite problem, increasing the safety of “rocking chair” LIBs. Building on this successful experience with LIBs, the fabrication of zinc-free “rocking chair” ZIBs may potentially disrupt the bottleneck of zinc metal anodes. This study aims to discover suitable anode materials that can accommodate reversible zinc ion plating and stripping. Research has identified four major types of anode materials for ZIBs: transition metal oxides, transition metal sulfides, MXene composites, and organics compounds, which are demonstrated to be excellent anode materials for ZIBs.

3.1. Transition metal oxides

Examining the possibility of using new anode materials in ZIBs is crucial. Replacing the zinc metal plates in ZIBs with anodes capable of storing zinc ions at low potentials through an intercalation mechanism is reasonable. MoO_x ($x = 2, 3$) is an attractive anode material that has been studied in batteries.

Hexagonal MoO_3 with a discharging potential of 0.36 V vs. zinc ions/zinc was studied as the anode for ZIBs (Fig. 3(a)) [51]. Ions are highly likely to transfer and diffuse through the channels, cavities, and grain boundaries in the hexagonal MoO_3 (h- MoO_3) skeleton (Fig. 3(b)), leading to superior stability and fast transfer dynamics. Equipped with an h- MoO_3 anode and a $\text{Zn}_{0.2}\text{MnO}_2$ cathode, a full cell named h- $\text{MoO}_3//\text{Zn}_{0.2}\text{MnO}_2$ was assembled. The cycling behavior of

h-MoO₃//Zn_{0.2}MnO₂ cells was investigated by constant current charge–discharge measurements at 1 A·g⁻¹. The cell demonstrates remarkable stability for maintaining over 100% of its initial capacity at 1000 cycles (Fig. 3(c)). The insertion of protons in layered MoO₃ can cause serious structural damage during cycling, hindering its use in diluted acidic electrolytes. The electrochemical conduct of MoO₃ anodes in electrolytes containing ZnCl₂ was improved to enhance the stabilities of proton storage in acidic media (Fig. 3(d)) [61]. X-ray diffraction (XRD) results showed that the synthesized α-MoO₃ has a stable layered orthorhombic structure with a

space group of *Pbnm* (JCPDS No. 35-0609). Thermodynamically, the stable MoO₃ morphology comprises a bilayer of MoO₆ octahedra (Fig. 3(e)). The electrochemical proton storage behavior was significantly improved using MoO₃ anode in 20 M ZnCl₂ + 1 M HCl electrolyte. Combined with the Ni-PBA cathode, the rate performance of the cell was investigated. The discharge capacity at 1 A·g⁻¹ is 47.9 mAh·g⁻¹, and after resetting to 1 A·g⁻¹, the discharge capacity is 76.1% of its original capacity, indicating a well-cycled performance of 99.5% coulombic efficiency (CE) after 400 cycles (Fig. 3(f)).

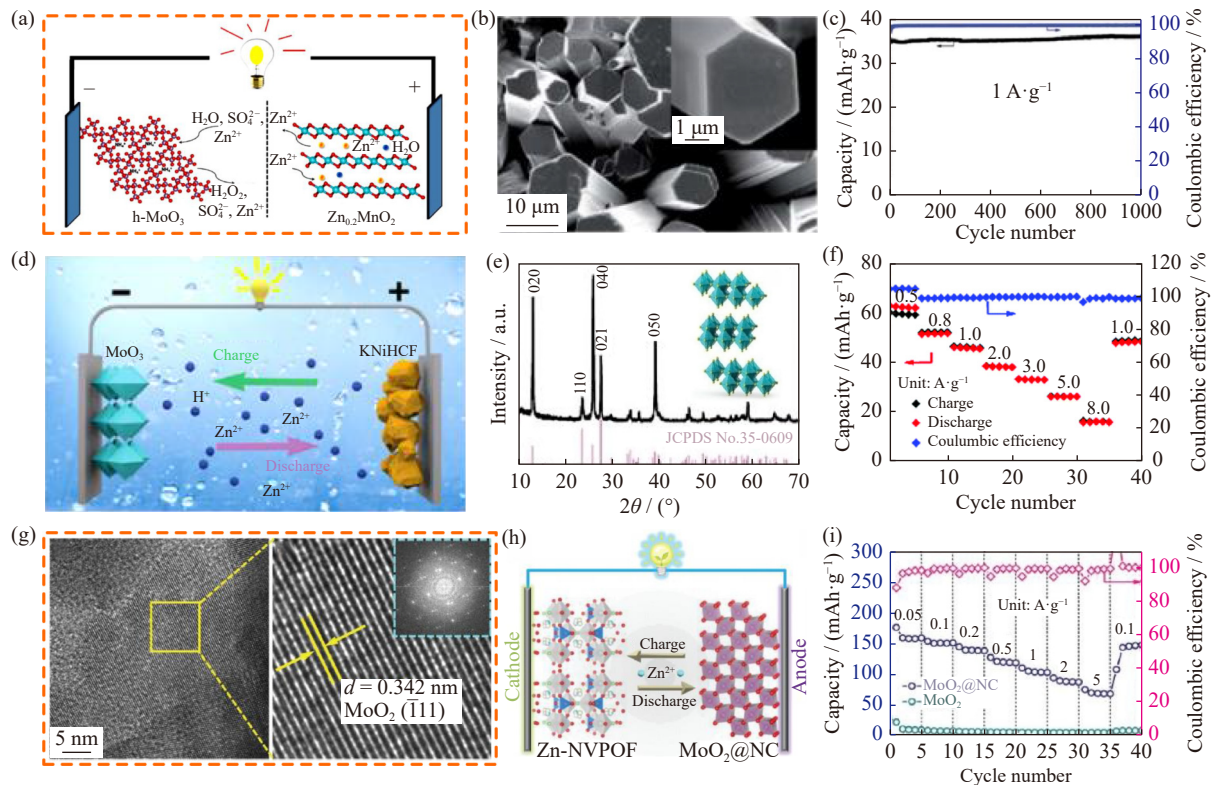


Fig. 3. (a) Schematic of the h-MoO₃//Zn_{0.2}MnO₂ battery; (b) scanning electron microscopy (SEM) of as-prepared h-MoO₃; (c) cycling performance of h-MoO₃//Zn_{0.2}MnO₂ battery; (d) schematic of the rocking chair aqueous hydrogen-ion battery; (e) XRD and typical crystal structure of as-prepared MoO₃; (f) rate performance of aqueous hydrogen-ion battery; (g) high resolution transmission electron microscope (HRTEM) images of MoO₂@NC; (h) schematic of MoO₂@NC//Zn-NVPOF cell; (i) rate capability at various current densities. (a–c) Reproduced from Ref. [51] with permission from the Royal Society of Chemistry. (d–f) Reproduced from Ref. [61] with permission from the Royal Society of Chemistry. (g–i) B. Wang, J.P. Yan, Y.F. Zhang, M.H. Ye, Y. Yang, and C.C. Li, *Adv. Funct. Mater.*, vol. 31, art. No. 2102827 (2021) [48]. Copyright Wiley-VCH Verlag GmbH & Co. KGaA. Reproduced with permission.

The MoO₂ materials, with their metallic characteristics of high theoretical capacity, a narrow band gap, and low resistivity, as well as new 1D tunnels for fast ion transport, can potentially be used as an anode for ZIB. However, the structure degradation and inherent kinetics during ion intercalation–deintercalation hinder its electrochemical performance. Therefore, a new nitrogen-doped carbon-embedded MoO₂ (MoO₂@NC) material with an interlayer structure was developed using a combined interlayer process and *in situ* carbonization of aniline [48]. The apparent lattice stripe of MoO₂@NC can be observed under HRTEM (Fig. 3(g)), demonstrating a *d*-spacing measurement of 0.342 nm, which agrees with the (111) plane of monoclinic MoO₂ crystals. An

apparently selective electron diffraction pattern of MoO₂@NC confirms its high crystallinity. The rocker-type zinc ion full cell comprised a zinc pre-inserted layer Na₃V₂(PO₄)₂O₂F anode (Fig. 3(h)), and the laminated MoO₂@NC also exhibits superior rate performance compared to pure MoO₂ (Fig. 3(i)). The capacity of the reversible discharge can be quickly returned to 147 mAh·g⁻¹ when the current density is shifted back to 0.1 A·g⁻¹, indicating that the MoO₂@NC electrode maintains good cycling reversibility after operating at high current densities. The long cycle stabilization is also an index in the merit evaluation of ZIB anode materials. The MoO₂@NC electrode can sustain a capability of 43 mAh·g⁻¹ after 3000 cycles at 5 A·g⁻¹.

The tunnel-shaped electrodes with large interlayer distances are highly suitable for storing zinc ions. The suitability of these electrodes can be attributed to their capability to accommodate the large radius of hydrated zinc ions (4.30 Å) and overcome the strong electrostatic interactions between zinc ions and laminated structures. As a layered structure material with a large (110) layer spacing of 5.3 Å, WO₃ is a good candidate as an intercalation anode in rocking chair ZIBs. The properties of ion diffusion, conductivity, and structural stability can be improved through proper material coupling, which enhances the electrochemical plating/stripping behavior.

The (001) surface of WO₃ and ($\bar{1}10$) surface of WC were well-matched, forming a WO₃/WC heterojunction that was used as the intercalation anode (Fig. 4(a)) [47]. The prepared WO₃/WC has a flower-like morphology with uniform element distribution of W, O, and C (Fig. 4(b)). The stacked and evanescent WO₃ nanosheets have a large number of reactive sites and a wide range of oxidation states to store zinc ions.

Meanwhile, studies showed that the coupled WO₃ and WC can markedly increase ionic conductivity, facilitating the formation of thermodynamically steady interfaces. In the discharged process, two W⁵⁺ signals are observed in the W⁴⁺ spectrum while W⁶⁺ is decreasing (Fig. 4(c)), indicating the partial reduction of W⁶⁺ to W⁵⁺. Benefiting from the favorable interfacial energy and electronic coupling as well as the significant charge transfer between WO₃ and WC, the electrochemical mechanism of zinc ion storage is shown in Fig. 4(d). WO₃/WC has the capacity of 164 mAh·g⁻¹ and cyclability of 90.2%. h-WO₃/3DG was researched as an insert anode for ZIBs [60]. The large surface area and electronic conductivity of porous graphene effectively contribute to the wetting of the electrolyte and increase the electrochemical dynamics of h-WO₃. The zinc-free metal full cell was constructed with h-WO₃/3DG as the anode and ZnMn₂O₄/CB as the cathode (Fig. 4(e)), showing a high capacity of 66.8 mAh·g⁻¹ at 0.1 A·g⁻¹.

A novel microwave-assisted chemical insertion technique

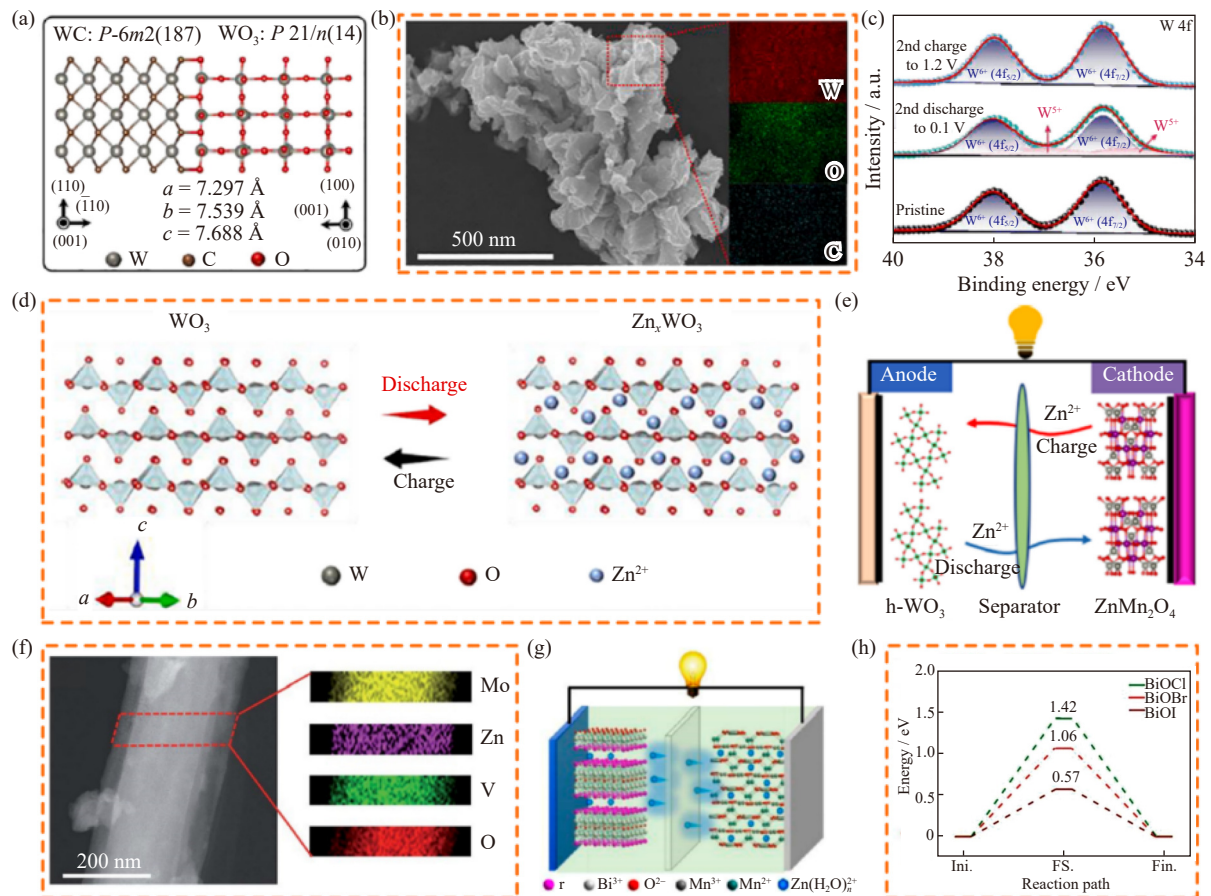


Fig. 4. (a) Schematic structure of WO₃/WC heterogeneous hybrid; (b) SEM figures of WO₃/WC hybrid; (c) W 4f spectra of WO₃/WC; (d) the electrochemical mechanism of zinc ion storage in WO₃/WC heterogeneous hybrid; (e) structural illustrations of the h-WO₃/3DG//ZnMn₂O₄/CB full battery; (f) scanning transmission electron microscopy (STEM) image with EDS mapping of the zinc-inserted compound Zn_xMo_{2.5+y}VO_{9+tz} ($x = 1$); (g) structural illustration of BiOI//Mn₃O₄ battery; (h) energy profiles of the corresponding Zn diffusion pathways. (a–d) Reprinted from *Chem. Eng. J.*, 426, J. Cao, D.D. Zhang, Y.L. Yue, et al., Strongly coupled tungsten oxide/carbide heterogeneous hybrid for ultrastable aqueous rocking-chair zinc-ion batteries, art. No. 131893, Copyright 2021, with permission from Elsevier [47]. (e) Reprinted with permission from X.F. Chen, R.S. Huang, M.Y. Ding, H.B. He, F. Wang, and S.B. Yin, *ACS Appl. Mater. Interfaces*, vol. 14, 3961–3969 (2022) [60]. Copyright 2022 American Chemical Society. (f) Reproduced from Ref. [41] with permission from the Royal Society of Chemistry. (g, h) Reprinted with permission from Q. Zhang, T.F. Duan, M.J. Xiao, et al., *ACS Appl. Mater. Interfaces*, vol. 14, 25516–25523 (2022) [49]. Copyright 2022 American Chemical Society.

was adopted to solve the problems of zinc dendrites in ZIBs. Zinc ions were inserted into the open tunnel oxide matrix to form a high-performance plug-in zinc composite anode $Zn_xMo_{2.5+y}VO_{9+z}$ [41]. Ultrafine chemical insertion of zinc was obtained using diethylene glycol and $Zn(CH_3COO)_2$ in an environmental atmosphere for 30 min. STEM and energy dispersive X-ray spectroscopy (EDS) analysis were used to assess the single particles of $Zn_xMo_{2.5+y}VO_{9+z}$ ($x = 1$). Zn, Mo, V, and O are found to be uniformly distributed over the entire particle with a low-surface zinc concentration. This finding proves that zinc ions are inserted into the $Mo_{2.5+y}VO_{9+z}$ channel (Fig. 4(f)). The results showed that the crystal morphology and crystallinity of the zinc intercalation remain unchanged. Unit cell swelling associated with zinc content was observed. As an insertion anode, $Zn_xMo_{2.5+y}VO_{9+z}$ ($x = 1$) can be successfully applied in aqueous and non-aqueous electrolytes with excellent electrochemical properties. The development of high capacity intercalated anode is the key to driving the development of ZIBs [49]. The interlayer distance and low zinc ion diffusion barrier obtained by density functional theory (DFT) are considered to be promising for electrodes, and a stand-alone BiOI nanopaper was designed (Fig. 4(g)). DFT shows that the diffusion potential resistance of zinc ions in BiOI (0.57 eV) is smaller than that of BiOCl and BiOBr (Fig. 4(h)). When the same number of zinc ions was inserted into BiOX, the interlayer distance of BiOI changes the least, indicating that BiOI has excellent structural stability during the insertion–deinsertion process of zinc ions. These experimental results manifest that the battery has a high initial capacity when combined with the Mn_3O_4 cathode.

3.2. Transition metal sulfides

Intercalation anodes are a promising solution to overcome the challenges associated with conventional ZIBs. However, only a few host materials exhibit electrochemical intercalation of zinc ions. $M_xMo_6T_8$ ($M = \text{metal}$, and $T = \text{S, Se, or Te}$) is one of the most attractive electrochemical multivalent ion intercalation host materials due to its strong chemical intercalation capability for metals, such as Mg, Ca, Ba, and Zn.

The $Zn_xMo_6S_8$ ($x = 0, 1, 2$) phase has received attention as a potential electrode material for ZIBs because Mo_6S_8 is known to intercalate zinc ions electrochemically. $Zn_xMo_6S_8$ was prepared by inserting zinc ions, and its crystal structure was characterized [42]. A six-membered ring is formed by the symmetrically generated Zn1 position (Fig. 5(a)–(b)). The interatomic distances of Zn1–Zn1 are 1.076, 1.838, and 2.130 Å, which are all excessively short for the metal–metal distance. If any position is filled at a given time, then only one of the six positions should be occupied, limiting the maximum occupancy to 1/6. Fig. 5(c) shows the average Mo–Mo interatomic distances. A large portion of the inserted zinc ions was trapped in the Zn1 site, yielding a first-cycle irreversible capacity of 134 $\text{mAh}\cdot\text{g}^{-1}$ at 0.05C of approximately 46 $\text{mAh}\cdot\text{g}^{-1}$. Synthetic Mo_6S_8 can be used as an anode material for ZIBs (Fig. 5(d)) [62]. The resulting Mo_6S_8 particles have defined cubic shapes with an average size of 100 nm

(Fig. 5(e)). The full cell is assembled by integrating the Mo_6S_8 electrode with a cathode based on poly (zinc iodide). The Γ/I^{3-} has a standard potential of 0.536 V for standard hydrogen electrode (SHE), which has a strong potential for real applications. The full cell was assigned as a static h-cell using a cation exchange membrane (CEM) due to the distinctive electrochemical properties of the cathode electrolyte (Fig. 5(f)). The cathode uses the ZnI_2 and I_2 , and the electrolyte uses $ZnSO_4$ on the anode side. Furthermore, the anode reaction of this filled cell occurs at a charge–discharge plateau of 0.35 V.

Instead of metallic zinc anode, samples with different charge states were analyzed by taking an intercalation type anode material to determine the zinc content in zinc hexacyanoferrate $K_x(H_2O)_{0.22}Zn_3[Fe(CN)_6]_2$ (named as ZPB) during the insertion–deinsertion process [63]. The analysis results were consistent with the zinc content calculated on the basis of the discharge–charge capacity. Additionally, the electrode mapping for complete discharge showed a uniform distribution of zinc atoms in the particles (Fig. 5(g)). The crystal structure of $Zn_{0.72}ZPB$ was defined and improved by crystallographic techniques, specifically inserting the position and environment of the zinc ion (Fig. 5(h)). The cell uses $Zn_2Mo_6S_8$ as the anode and ZPB as the cathode in $ZnSO_4$ electrolyte (Fig. 5(i)). The demonstration cell was designed with a cathode limited with a negative/positive (N/P) mass ratio of 5.5:1, minimizing the impact of the anode material. The assembled full cell exhibits a cycle capacity of 62.3 $\text{mAh}\cdot\text{g}^{-1}$ and an average discharge voltage of 1.40 V.

Research efforts have focused on the development of intercalation anodes that can reversibly and rapidly accommodate divalent zinc ions. One effective strategy is the use of anode materials with reasonable tunnel structure or large interlayer distance. As a typical layered material, a new type of pre-precipitated TiS_2 is proposed and used as an intercalation anode [43]. The XRD spectrum of TiS_2 (Fig. 6(a)) confirms the synthesis of pure TiS_2 with no impurities because all peaks are effectively indexed to TiS_2 . The inset in Fig. 6(a) shows the typical crystal structure of TiS_2 along the (100) direction. The full cell was developed using $Na_{0.14}TiS_2$ and $ZnMn_2O_4$ as the cathode and anode, respectively (Fig. 6(b)). Fig. 6(c) depicts the rate capacity of $Na_{0.14}TiS_2$ in the current density range from 0.05 to 2 $\text{A}\cdot\text{g}^{-1}$. The capacity of the $Na_{0.14}TiS_2$ electrode is 140 $\text{mAh}\cdot\text{g}^{-1}$ at a low current density of 0.05 $\text{A}\cdot\text{g}^{-1}$, and the capacity is maintained at 120, 103, 84, 70, and 58 $\text{mAh}\cdot\text{g}^{-1}$ at 0.1, 0.2, 0.5, 1, and 2 $\text{A}\cdot\text{g}^{-1}$, respectively, indicating its promising fast charge–discharge capability.

The development of intercalated anodes is a promising approach to overcome the limitations of conventional zinc anodes. However, their application is hampered by the low capacity due to the limited number of electrons transferred by the intercalation reaction. Cu^+ -based materials are proven effective for conversion reactions. These materials have a large capacity and can improve energy density. The cetyltrimethylammonium bromide (CTMAB) pre-inserted CuS with increased interlayer spacing ($CuS@CTMAB$) as high capa-

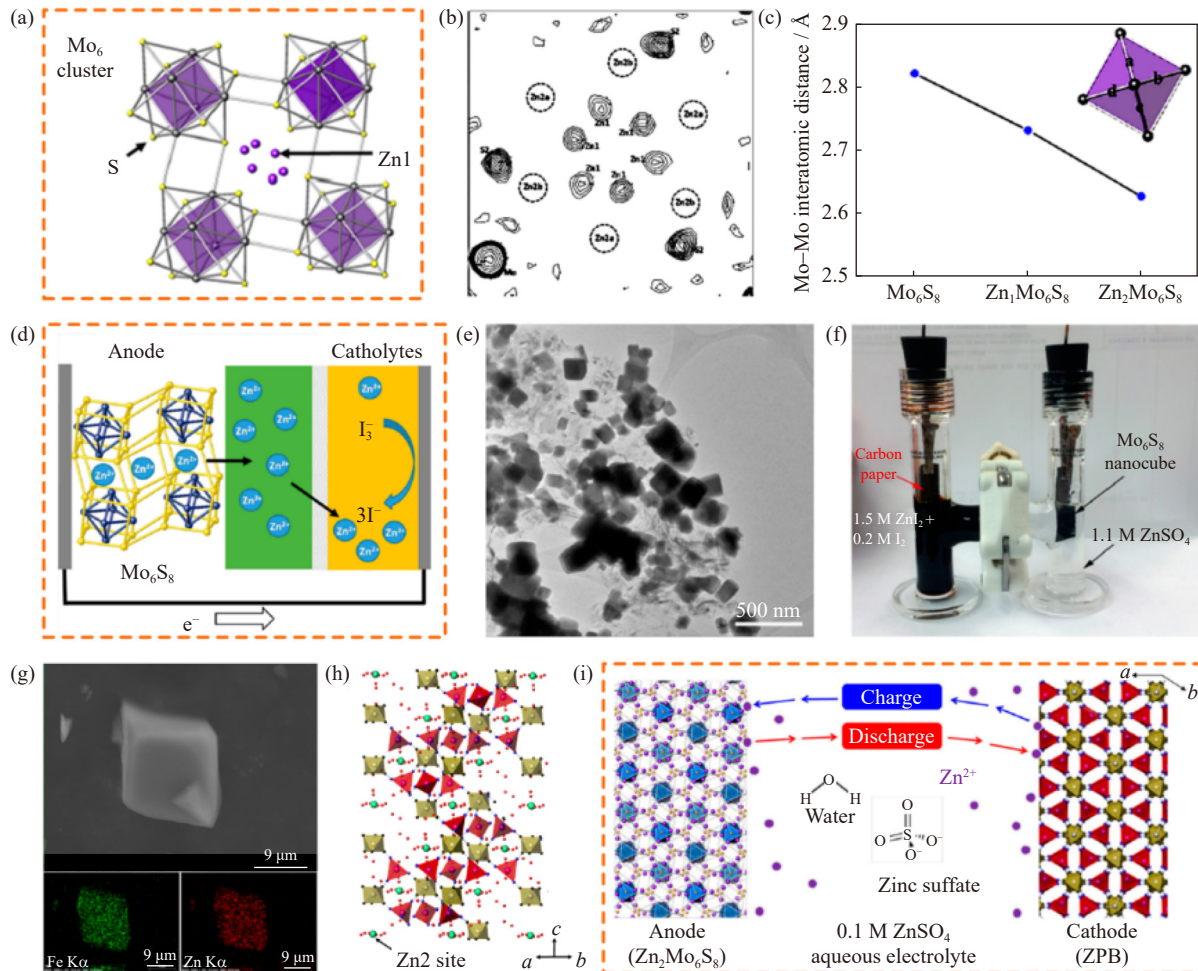


Fig. 5. (a) Local structure around the Zn1 positions in ZnMo_6S_8 ; (b) (001) sections of the observed Fourier map; (c) average interatomic distances of Mo–Mo; (d) structural illustration of ZIBs; (e) transmission electron microscope (TEM) of Chevrel phase nanocubes; (f) photograph of the full cell (a CEM was used to separate the cathode electrolyte from the anode electrolyte); (g) EDX elemental mapping of $\text{Zn}_{0.72}\text{ZPB}$; (h) crystal structure of $\text{Zn}_{0.72}\text{ZPB}$; (i) illustration of the compositions for the rocking chair ZIBs. (a–c) Reprinted with permission from M.S. Chae, J.W. Heo, S.C. Lim, and S.T. Hong, *Inorg. Chem.*, vol. 55, 3294–3301(2016) [42]. Copyright 2016 American Chemical Society. (d–f) Reprinted with permission from Y.W. Cheng, L.L. Luo, L. Zhong, et al., *ACS Appl. Mater. Interfaces*, vol. 8, 13673–13677 (2016) [62]. Copyright 2016 American Chemical Society. (g–i) Reprinted from [63].

city anode material [64]. The insertion of zinc ions into Cu forms multiple electron aggregation regions near Cu and S atoms, which could be local internal electric fields for Cu and S atoms and promote the atoms for rapid charge transport (Fig. 6(d)). Various characterizations were also performed to further investigate the storage mechanism of zinc ions in CuS@CTMAB during electrochemical charge and discharge. The uniform distribution of zinc elements in the mapping of fully discharged Cu@CTMAB electrodes visually verifies the successful insertion of zinc ions (Fig. 6(g)). The CuS@CTMAB as the anode is used to establish the cell system. The actual capacity of the CuS@CTMAB//ZMO cell is $201.9 \text{ mAh}\cdot\text{g}^{-1}$ (Fig. 6(e)), and the capacity is limited by the CuS anode. The CuS@CTMAB anode can provide a high reversible capacity of $211.1 \text{ mAh}\cdot\text{g}^{-1}$ after 100 cycles with an average CE of 99.3%. Furthermore, the CuS@CTMAB electrodes demonstrated long-term cycling stability, maintaining 61.1% capacity after 3000 cycles (Fig. 6(f)).

The unique properties of mixed-valence Cu_{2-x}Se , such as its rigid bulk structure, rich electron cation sites, and excel-

lent conductivity, increase its effectiveness as an anode material for ZIBs. Long-lasting zinc-free metal rocker ZIBs were constructed using mixed-valence Cu_{2-x}Se as the anode [45]. The charge storage mechanism must be understood to explain the electrochemical performance of mixed-valence Cu_{2-x}Se over CuSe. The DFT showed that the introduction of low-valent Cu not only changes the active site for zinc ion storage but also optimizes the electronic interaction, resulting in an intercalation formation energy of -0.68 eV and a low diffusion potential barrier (Fig. 7(a)). The ZIBs using mixed-valence Cu_{2-x}Se anode and a commercial MnO_2 cathode were investigated. The Cu_{2-x}Se nanorod anode has a cubic structure that promotes fast electron transport, which enhances the electrode kinetics with high capacity, CE, and stable electrochemical cycling. The fabricated $\text{Zn}_x\text{MnO}_2//\text{Cu}_{2-x}\text{Se}$ full cell exhibits remarkable electrochemical performance (Fig. 7(b)), including a long cycle life of over 20000 cycles at a current density of $2 \text{ A}\cdot\text{g}^{-1}$.

TiSe_2 has a large interlayer spacing (0.601 nm) and high electronic conductivity, enabling fast ion (de)intercalation

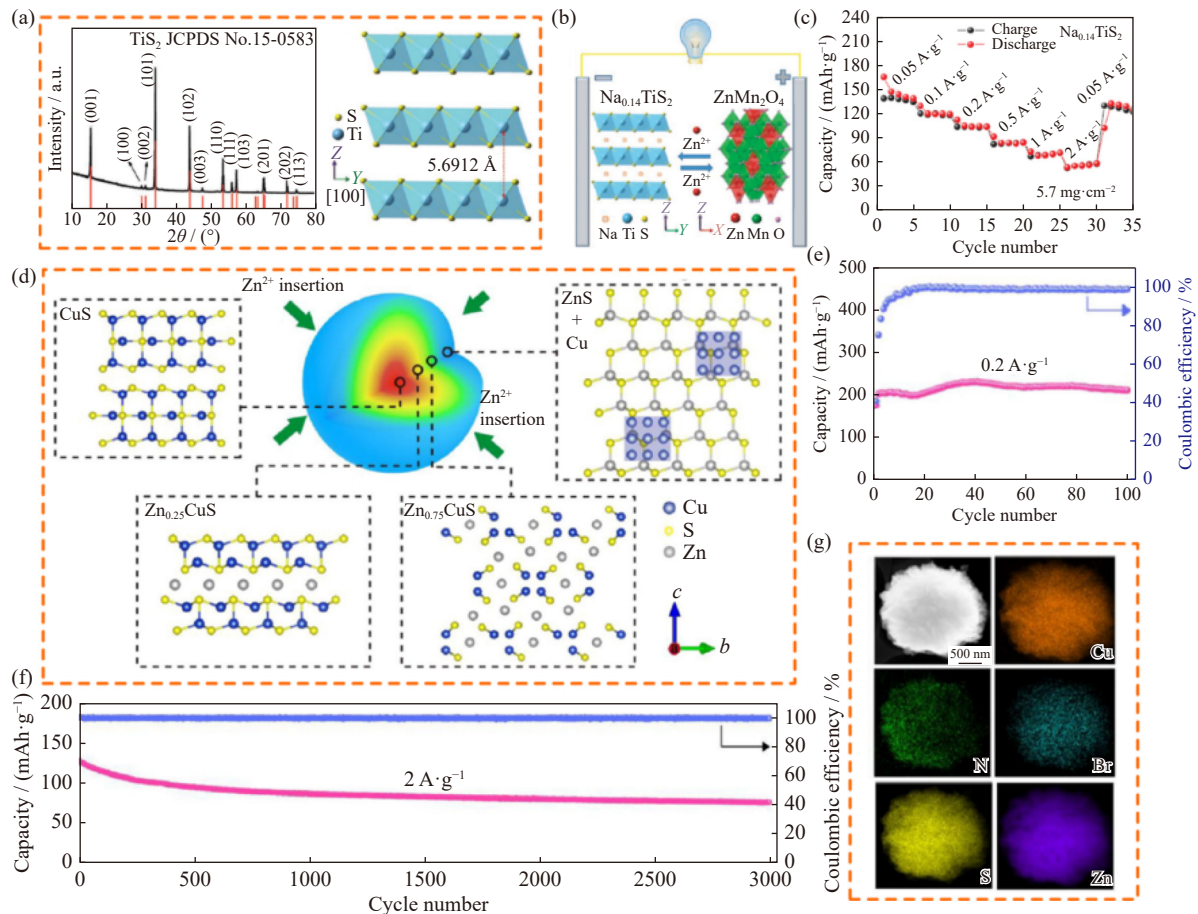


Fig. 6. (a) XRD pattern and crystallographic structure of TiS_2 ; (b) structural illustrations of $\text{Na}_{0.14}\text{TiS}_2//\text{ZnMn}_2\text{O}_4$ battery; (c) rate capacities of $\text{Na}_{0.14}\text{TiS}_2$; (d) schematic illustration of the reaction pathway of zinc ions in CuS ; (e) cycling performance of the $\text{CuS@CTMAB}/\text{ZMO}$ cell; (f) cycling performance of the CuS@CTMAB ; (g) mapping of the CuS@CTMAB after its discharge to 0.3 V in the initial cycle. (a–c) An ultrastable presodiated titanium disulfide anode for aqueous “rocking-chair” zinc ion battery, *Adv. Energy Mater.*, vol. 9, art. No. 1900993 (2019) [43]. Copyright Wiley-VCH Verlag GmbH & Co. KGaA. Reproduced with permission. (d–g) Reprinted with permission from Z.H. Lv, B. Wang, M.H. Ye, Y.F. Zhang, Y. Yang, and C.C. Li, *ACS Appl. Mater. Interfaces*, vol. 14, 1126–1137 (2022) [64]. Copyright 2022 American Chemical Society.

and electron transport [65]. The layered structure of TiSe_2 increases its suitability as an anode in ZIBs (Fig. 7(c)). The interlayer spacing is 0.601 nm in the TEM image (Fig. 7(d)), corresponding to the (001) side of TiSe_2 . The mapping of the randomly selected region in Fig. 7(e) shows a uniform distribution of Ti and Se elements. The ZIBs full cell prepared from TiSe_2 anode and VO_2 cathode has a capacity of 44.3 $\text{mAh}\cdot\text{g}^{-1}$ at 0.20 $\text{A}\cdot\text{g}^{-1}$. *In situ* electrochemical activation of Cu_{2-x}Te proved its potential as an anode material for ZIBs [46]. The $\text{Cu}_{2-x}\text{Te}/\text{Na}_3\text{V}_2(\text{PO}_4)_3$ cell is validated owing to the dendrite-free anode, the suitable potential, and the robust structure of Cu_{2-x}Te (Fig. 7(f)). The electrochemical synthesis of Cu_{2-x}Te is shown in Fig. 7(g). The energy density is 58 $\text{Wh}\cdot\text{kg}^{-1}$, the average voltage is 0.98 V, and 92% capacity is maintained after 1000 cycles of C/2. Layered TiTe_2 prepared by a one-step vacuum sintering technique was used as a zinc metal-free anode for ZIBs, solving the existing problem of zinc metal [66]. DFT and *ab initio* molecular dynamics (AIMD) simulations, which predicted the layered TiTe_2 , were also used as a zinc metal-free anode, demonstrating high thermodynamic stability and good ion migration kinetics. The half-cell with a working electrode of TiTe_2 has 225

$\text{mAh}\cdot\text{g}^{-1}$ at 0.1 $\text{A}\cdot\text{g}^{-1}$ and excellent cycling stability.

3.3. MXene composite material

MXene, a 2D transition metal carbide, has gained significant attention due to its excellent mechanical strength, metallic conductivity, and ion adsorption capability. MXene has the formula $\text{M}_{n+1}\text{X}_n\text{T}_x$ ($n = 1, 2, 3$), where M is the transition metal, X is C or N, and T_x is the surface terminus ($-\text{OH}$, $-\text{O}$, or $-\text{F}$). MXene is a promising candidate for anode materials for ZIBs due to its excellent electronegativity, metal conductivity, and stable cycling behavior.

The ultrathin NHVO nanoribbons (approximately 14 nm) effectively contact $\text{Ti}_3\text{C}_2\text{T}_x$ substrates and act as a fast ion transport nanosheet interlayer, which prevents $\text{Ti}_3\text{C}_2\text{T}_x$ aggregation [50]. A schematic describing the charge storage mechanism of the $\text{NHVO@Ti}_3\text{C}_2\text{T}_x$ hybrid membrane electrode for zinc ions is shown in Fig. 8(a). The $\text{NHVO@Ti}_3\text{C}_2\text{T}_x$ hybrid membrane electrode demonstrates the potential for reversible embedding/de-embedding of zinc ions in the NHVO host and appearance/disappearance of the new phase (ZVOH) during the discharging/charging cycles. The cell capacitance of the $\text{NHVO@Ti}_3\text{C}_2\text{T}_x$ hybrid membrane

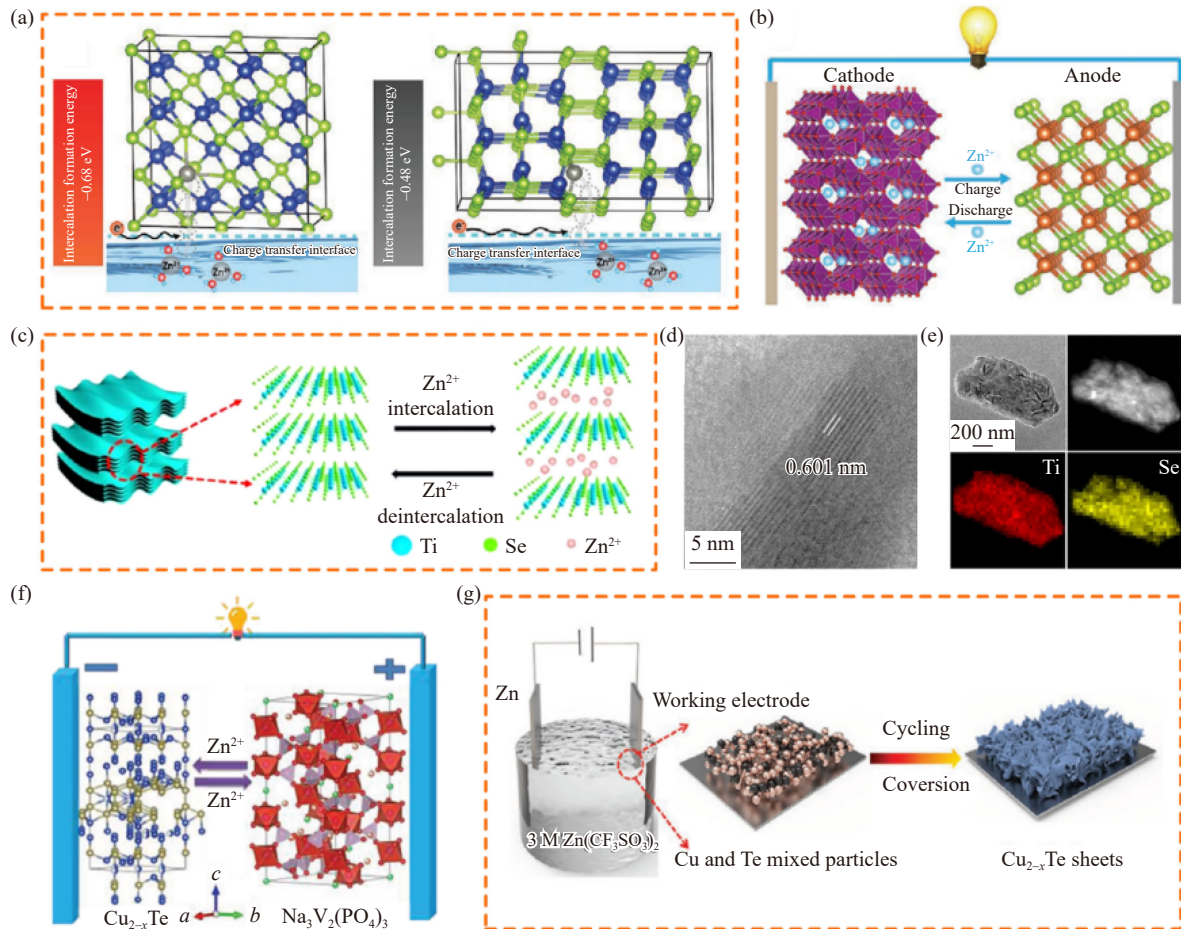


Fig. 7. (a) Charge transfer process and intercalation formation energy of Cu_{2-x}Se and CuSe at the reaction interface; (b) schematic of the $\text{Zn}_x\text{MnO}_2/\text{Cu}_{2-x}\text{Se}$ full battery; (c) structure and storage mechanism of TiSe_2 ; (d) TEM image of TiSe_2 ; (e) mapping images of the pristine TiSe_2 electrode; (f) structural illustration of $\text{Cu}_{2-x}\text{Te}/\text{Na}_3\text{V}_2(\text{PO}_4)_3$ full batteries; (g) synthetic illustration of Cu_{2-x}Te . (a, b) Y. Yang, J.F. Xiao, J.Y. Cai, *et al.*, *Adv. Funct. Mater.*, vol. 31, art. No. 2005092(2021) [45]. Copyright Wiley-VCH Verlag GmbH & Co. KGaA. Reproduced with permission. (c–e) Reprinted from *Nano Energy*, 93, L. Wen, Y.N. Wu, S.L. Wang, *et al.*, A novel TiSe_2 (de)intercalation type anode for aqueous zinc-based energy storage, art. No. 106896., Copyright 2022, with permission from Elsevier [65]. (f, g) W. Li, Y.S. Ma, P. Li, X.Y. Jing, K. Jiang, and D.H. Wang, *Adv. Energy Mater.*, vol. 11, art. No. 2102607(2021) [46]. Copyright Wiley-VCH Verlag GmbH & Co. KGaA. Reproduced with permission.

electrode was investigated using $\text{NHVO}@\text{Ti}_3\text{C}_2\text{T}_x$ and ZnMn_2O_4 as the anode and the cathode, respectively (Fig. 8(c)). Different cyclic voltammetry (CV) curves were taken to research the type of stored charge, and the peak of the CV curves gradually widened and the peak position slightly shifted (Fig. 8(b)).

The ZIBs were developed by combining an MXene- TiS_2 (de)intercalation anode, a multiwalled carbon nanotube-vanadium dioxide cathode, and a zinc sulfate-polyacrylamide hydrogel electrolyte [67]. The lateral size and thickness of TiS_2 were reduced through grinding in N-Methyl pyrrolidone, as demonstrated in TEM images before and after the process (Fig. 8(d)). The resistance of the cell cathode and anode at different locations was tested to avoid short and open circuits (Fig. 8(e)), and the ZIBs demonstrated excellent cycle life, retaining 99.7% of its initial capacity after 500 cycles.

3.4. Organic compounds

Organic molecular materials are attracting attention due to

their potential to store divalent cations attributed to their inherent ductility and soft lattice, which allows for easy ion intercalation through molecular reorientation. These characteristics make organic molecules a viable alternative to traditional inorganic electrode materials.

Dendritic-free ZIBs have been developed by using organic quinone instead of metal zinc as anode materials. A schematic of the full cell, which comprises ball-milled 9,10-Anthraquinone (AQ) as the anode and spinel ZnMn_2O_4 (ZMO) as the cathode, is shown in Fig. 9(a) [44]. The equation of the electrode redox reaction is shown in the middle of the inset. The rate capability and cycling stability of the full cell were evaluated at different current densities ranging from 0.2 to $6.4 \text{ A} \cdot \text{g}^{-1}$ (Fig. 9(b)). Dendrite-free organic anodes of perylene-3,4,9,10-tetracarboxylic diimide (PTCDI) were used to polymerize the surface of reduced graphene oxide (PTCDI/rGO) [68]. The synthesized PTCDI/rGO electrode not only overcomes the problem of zinc stripping/plating inhomogeneity and improves the stability of ZIBs (Fig. 9(c)) but also shows superior rate capability. The lowest unoccu-

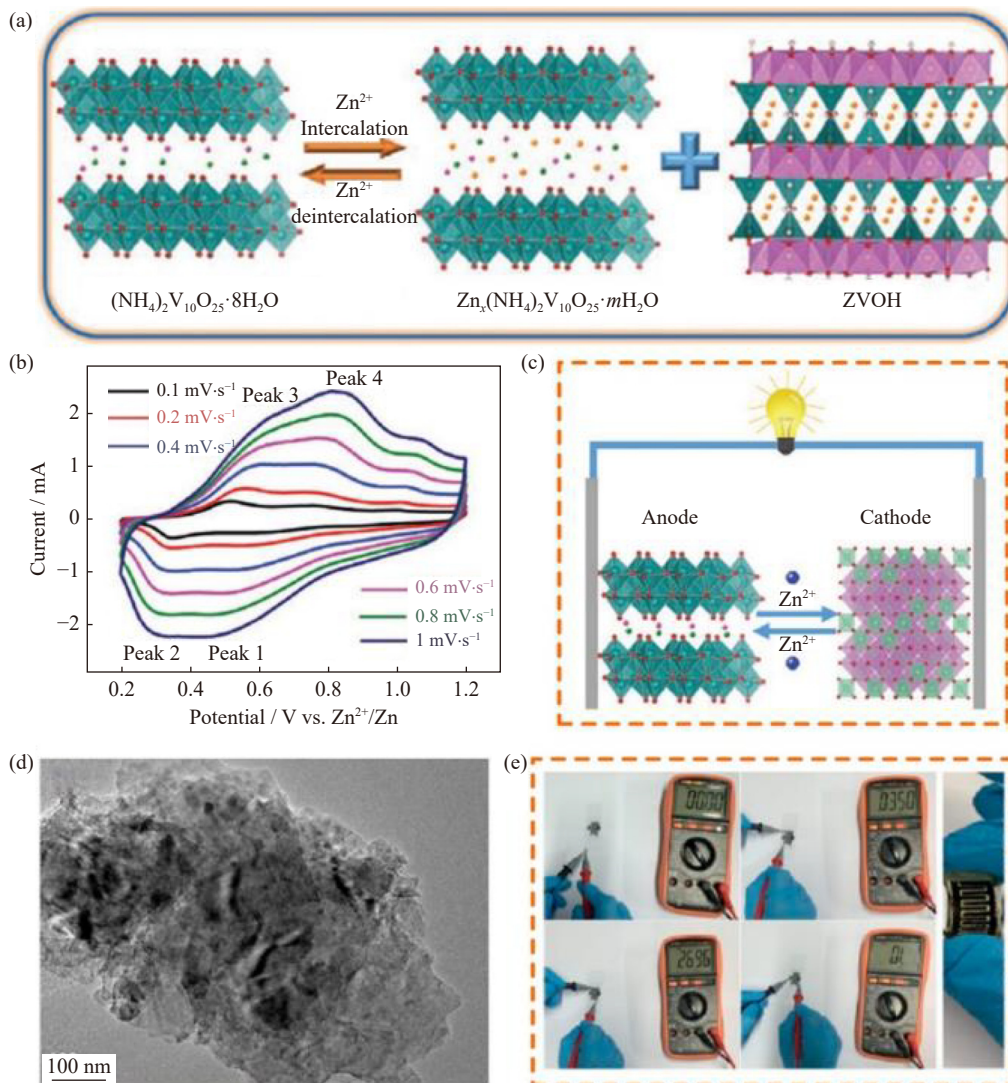


Fig. 8. (a) Storage mechanism diagram of zinc ions; (b) CV curves of the NHVO@Ti₃C₂T_x//ZnMn₂O₄ full battery; (c) schematic of NHVO@Ti₃C₂T_x//ZnMn₂O₄ full battery; (d) TEM image of the ground TiS₂; (e) resistance of the finger-like electrode at different positions. (a–c) X. Wang, Y.M. Wang, Y.P. Jiang, *et al.*, *Adv. Funct. Mater.*, vol. 31, art. No. 2103210 (2021) [50]. Copyright Wiley-VCH Verlag GmbH & Co. KGaA. Reproduced with permission. (d, e) Reprinted from *J. Power Sources*, 504, B.T. Zhao, S.L. Wang, Q.T. Yu, *et al.*, A flexible, heat-resistant and self-healable “rocking-chair” zinc ion microbattery based on MXene-TiS₂ (de)intercalation anode, art. No. 230076, Copyright 2021, with permission from Elsevier [67].

plied molecular orbital (LUMO) energy was calculated by applying DFT (Fig. 9(d)) to understand why this electrode potential is different from other conventional organic electrodes effectively, indicating that the redox potential is correlated with the LUMO energy level. PTCDI was found to have the highest LUMO energy level, corresponding to the lowest discharge potential.

Compared to other candidate materials, H₂Ti₃O₇·xH₂O film (HTOF) can significantly increase the working voltage level for its ultralow potential in ZIBs [69]. The apparent phenomenon between the HTOF and Na₂Ti₃O₇ electrodes suggests that the large lattice spacing between the layers and the crystal water is the key factor in stimulating the insertion of zinc ions into the low potential H₂Ti₃O₇·xH₂O (Fig. 9(e)). The enlarged lattice spacing and interlayer crystal water stimulate the co-insertion and extraction of zinc ions and H⁺ at the H₂Ti₃O₇·xH₂O anode. The low potential H₂Ti₃O₇·xH₂O

anode exhibits attractive cycle performance and CE assisted by interlayer crystal water. An aqueous phase zinc ion full cell was successfully formed using ZMO and HTOF as the anode and cathode, respectively (Fig. 9(f)), and the Zn_xMnO₂/H₂Ti₃O₇·xH₂O cell demonstrated good electrochemical performance (Fig. 9(g)).

3.5. Other zinc metal-free anodes

The zinc anode in ZIBs is a hostless electrode where zinc ions are plating/stripping at the electrode–electrolyte interface, resulting in the formation of segregated metal zinc during cycling and low cycling efficiencies. This process leads to the growth of zinc dendrites, causing unpredictable short circuits in the cell. Various methods, such as epitaxial electrodeposition, high salt concentration, and zinc surface coating, have been investigated to improve the cycling stability of ZIBs. ZIBs with activated carbon, bromobenzene, and inact-

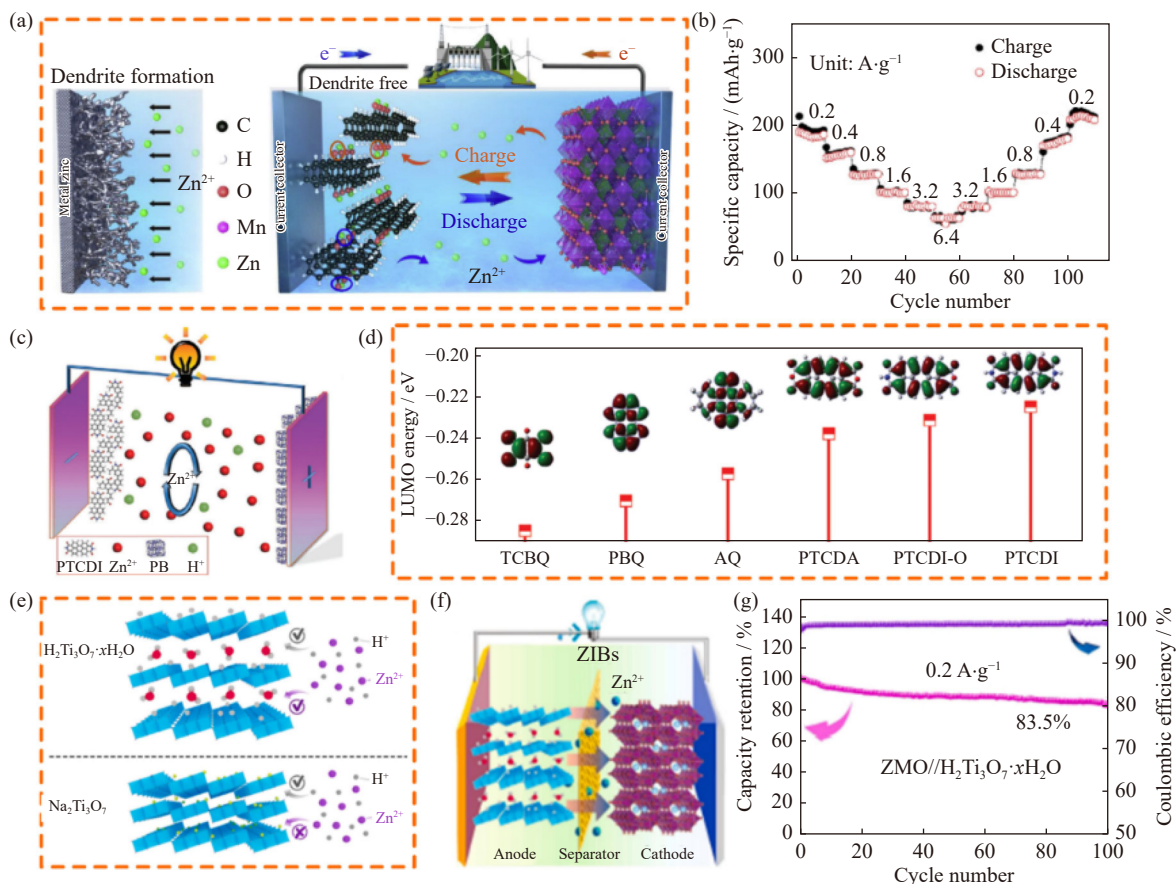


Fig. 9. (a) Schematic drawing of the working mechanism in ZIBs; (b) rate performance under different current densities; (c) schematic of the full battery; (d) LUMO energy levels calculated by DFT; (e) schematic of ion migration; (f) schematic illustration of ZMO//H₂Ti₃O₇·xH₂O full cell; (g) cycling performance of ZMO//H₂Ti₃O₇·xH₂O full cell (ZMO represents Zn_xMnO₂). (a, b) Reprinted from *Mater. Today Energy*, 13, L.J. Yan, X.M. Zeng, Z.H. Li, et al., An innovation: Dendrite free quinone paired with ZnMn₂O₄ for zinc ion storage, 323-330, Copyright 2019, with permission from Elsevier [44]. (c, d) N.N. Liu, X. Wu, Y. Zhang, et al., *Adv. Sci.*, vol. 7, art. No. 2000146 (2020) [68]. Copyright Wiley-VCH Verlag GmbH & Co. KGaA. Reproduced with permission. (e-g) Reprinted from *Chem. Eng. J.*, 420, Y. Liu, X.M. Zhou, X. Wang, et al., Hydrated titanate as an ultralow-potential anode for aqueous zinc-ion full batteries, art. No. 129629, Copyright 2021, with permission from Elsevier [69].

ive materials (such as Cu foil) as anodes have shown promise in effectively controlling the growth of zinc dendrites.

The performance of bromobenzene as an anode for ZIBs was investigated using first-principles calculations [70]. Coronene, which is an analog of graphene, has been demonstrated to be an ideal anode for Ca, Mg, Na, and Li ion batteries. Calculations show that the binding energy between the coronene substrate and zinc ions was approximately 0.79 eV, with the binding energy decreasing with an increase in zinc content. The storage capacity of bromobenzene sheets for ZIBs was found to be up to 433 mA·h·g⁻¹, which highlights the importance of zinc storage performance for ZIBs. The adsorption behavior of zinc atoms on bromobenzene sheets was also systematically investigated. Fig. 10(a)–(b) shows the optimized geometry of 10 zinc atoms adsorbed on the bromobenzene sheet, which were organized into two layers after relaxation.

Current zinc-based battery anodes all use excess zinc, which reduces the energy density of the battery. Therefore, the anode-free zinc designed by a nanocarbon nucleation layer has been studied, and its electrochemistry has been proven to have high efficiency and stability in a certain current dens-

ity and plating capacity range [52] (Fig. 10(c)). Metallic zinc has high theoretical capacity and energy density. Thus, the anode-free design of AZIBs can significantly increase the energy density of the entire battery. The nucleation layer of carbon nanosheets is coated on a Cu foil. Copper foil is also used as a collector due to its stability in various electrolytes and reasonable cost. This nucleation layer aims to promote uniform galvanization and reduce the energy barrier of formation. The anode-free Zn–MnO₂ cell comprises Cu foil and Zn(CF₃SO₃)₂ as the collector fluid and the electrolyte, respectively (Fig. 10(d)). Compared to the large-scale zinc dendrites formed on the Cu substrate, the zinc deposits on C/Cu electrodes are arrays of neatly arranged nanosheets.

4. Summary and perspectives

ZIBs that utilize zinc metal-free anodes are one of the latest prospective energy storage equipment, which addresses the challenges of zinc dendrite formation and side reactions on zinc metal anodes. The development and optimization mechanism of zinc metal-free anodes are reviewed in this paper, and their comprehensive performance in ZIBs is

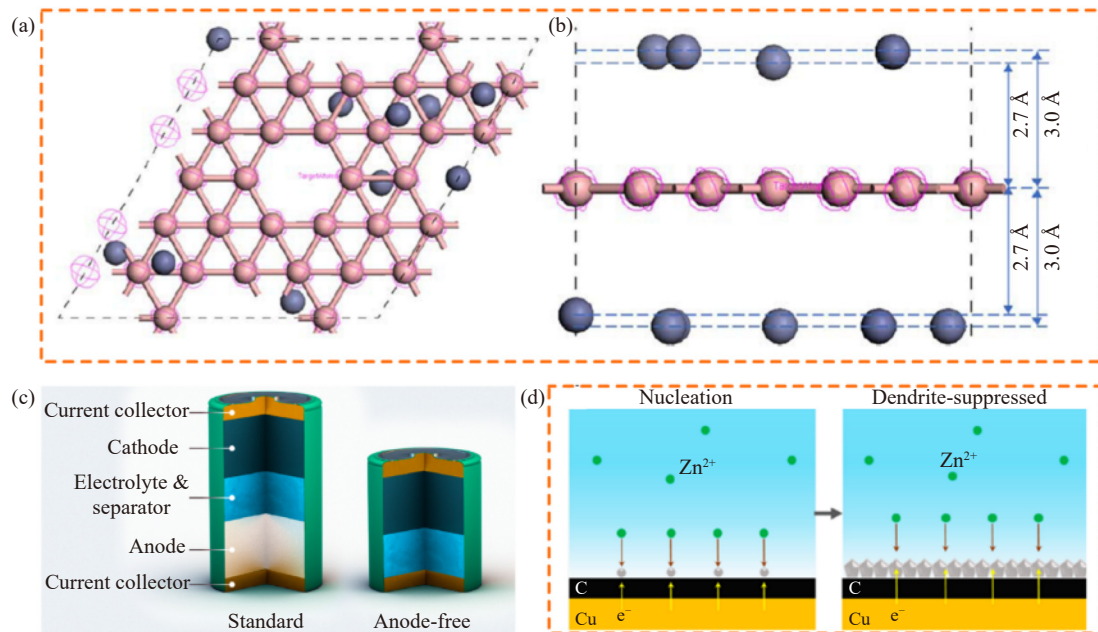


Fig. 10. (a, b) Geometry optimization of 10 zinc atoms attracted to a borophene sheet; (c) schematic of standard battery with metal anodes (e.g., Li, Na, Zn) and an anode-free battery; (d) diagram of zinc formation process on C/Cu electrode. (a, b) Reprinted from S.L. Leng, X.Y. Sun, Y.C. Yang, and R.H. Zhang, *Mater. Res. Express*, vol. 6, art. No. 085504 (2019) [70]. © IOP Publishing. Reproduced with permission. All rights reserved. (c, d) Reprinted with permission from Y.P. Zhu, Y. Cui, and H.N. Alshareef, *Nano Lett.*, vol. 21, 1446–1453 (2021) [52]. Copyright 2021 American Chemical Society.

illustrated. Four main categories of zinc metal-free anodes are as follows: transition metal oxides, transition metal sulfides, MXene composite material, and organic compounds. Other applications of zinc metal-free anodes in ZIBs, such as copper–carbon substrates and activated carbon materials, are

also described. Although zinc metal-free anodes hold considerable promise in ZIBs, further research is needed to improve the material properties and commercialization process. Herein, the authors provide some suggestions for advancing the development of zinc metal-free anodes in ZIBs (Fig. 11).

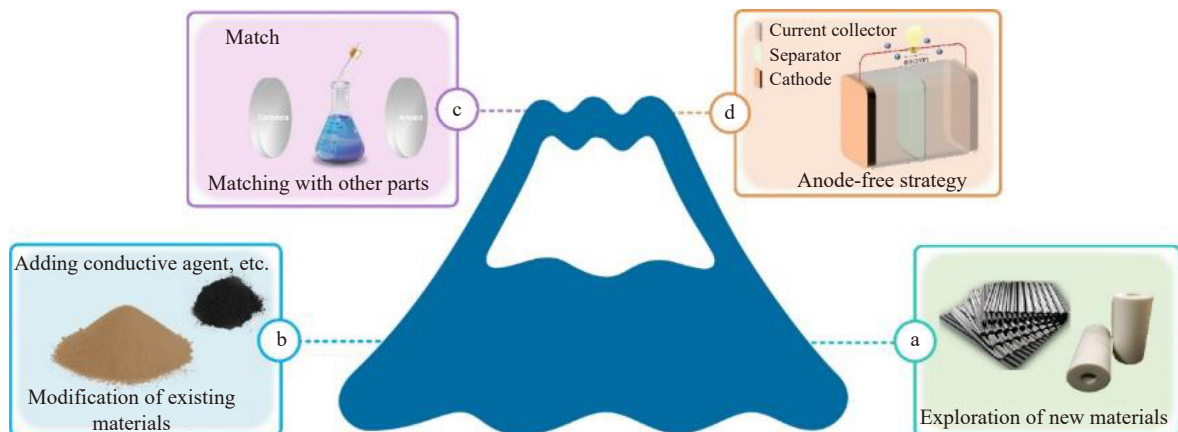


Fig. 11. Application prospect of zinc metal-free anodes.

(1) Exploration of new materials as zinc metal-free anodes. Research on metal-free zinc anodes remains in the beginning stages, and thus, exploring new materials is crucial. Some efforts have been provided in zinc metal-free anode research, including transition metal oxides, transition metal sulfides, MXene composites, and organic compounds. However, additional research is necessary before the commercialization of these materials. Further exploration of zinc-free metal anode materials is necessary to improve the anode performance.

(2) Rational optimization of existing materials. The op-

timization of zinc metal-free anode performance can be enhanced by combining existing materials with other components. Existing materials are more or less deficient in their performance, which affects their commercialization, and the compounding of existing materials with other materials can enhance these defects. For example, adding a conductive agent component can improve the charge transfer rate of anodes. Researchers should focus on optimizing the existing zinc metal-free anode materials based on the existing studies.

(3) Exploration of matched cathodes and electrolytes. The main challenge of the “rocking chair” ZIBs with a low

voltage window lies in the effect of the resultant depassivation and hydrogen evolution on the performance of battery electrode materials. A certain electrolyte possessing thermal stability, mechanical rigidity, and chemical stability should be investigated to overcome the aforementioned limitation. Different combinations of cathodes and anodes have varying requirements for the performance of the electrolyte due to the different redox potentials and energy storage mechanisms. Hence, exploring the most compatible cathode and electrolyte for commercialization and experimentation on ZIBs is crucial.

(4) Extension of anode-free strategy. The low capacity density of ZIBs is among their largest drawbacks due to the excessive mass of the zinc anode. Researchers have focused on electrolyte engineering to address this challenge by creating a stable mesophase that could adjust the zinc ion definition and guarantee a balanced deposition/solution of zinc at the collector interface. Therefore, anode-free ZIBs have emerged as promising candidates in energy storage applications owing to their high energy density, inherent security, low cost, and simplified manufacturing techniques.

Acknowledgements

This work was financially supported by the National Natural Science Foundation of China (Nos. 51872090 and 51772097), the Hebei Natural Science Fund for Distinguished Young Scholar, China (No. E2019209433), the Youth Talent Program of Hebei Provincial Education Department, China (No. BJ2018020), the Natural Science Foundation of Hebei Province, China (No. E2020209151), and the Science and Technology Project of Hebei Education Department, China (No. SLRC2019028).

Conflict of Interest

Zhangxing He is a youth editorial board member for IJMMM and was not involved in the editorial review or the decision to publish this article. All authors confirm that they have no competing interests or financial ties that could influence the outcomes or interpretation of this research.

References

- [1] B. Dunn, H. Kamath, and J.M. Tarascon, Electrical energy storage for the grid: A battery of choices, *Science*, 334(2011), No. 6058, p. 928.
- [2] M. Winter and R.J. Brodd, What are batteries, fuel cells, and supercapacitors?, *Chem. Rev.*, 104(2004), No. 10, p. 4245.
- [3] D. Larcher and J.M. Tarascon, Towards greener and more sustainable batteries for electrical energy storage, *Nat. Chem.*, 7(2015), No. 1, p. 19.
- [4] J.B. Goodenough and Y. Kim, Challenges for rechargeable Li batteries, *Chem. Mater.*, 22(2010), No. 3, p. 587.
- [5] J.M. Tarascon and M. Armand, Issues and challenges facing rechargeable lithium batteries, *Nature*, 414(2001), No. 6861, p. 359.
- [6] X. Guo, J. Zhou, C.L. Bai, X.K. Li, G.Z. Fang, and S.Q. Liang, Zn/MnO₂ battery chemistry with dissolution-deposition mechanism, *Mater. Today Energy*, 16(2020), art. No. 100396.
- [7] R.Y. Wen, Z.H. Gao, L. Luo, et al., Sandwich-structured electrospun all-fluoropolymer membranes with thermal shut-down function and enhanced electrochemical performance, *Nanocomposites*, 8(2022), No. 1, p. 64.
- [8] D.L. Chao, W.H. Zhou, C. Ye, et al., An electrolytic Zn–MnO₂ battery for high-voltage and scalable energy storage, *Angew. Chem. Int. Ed.*, 58(2019), No. 23, p. 7823.
- [9] F. Wang, O. Borodin, T. Gao, et al., Highly reversible zinc metal anode for aqueous batteries, *Nat. Mater.*, 17(2018), No. 6, p. 543.
- [10] Y. Song, P.C. Ruan, C.W. Mao, et al., Metal-organic frameworks functionalized separators for robust aqueous zinc-ion batteries, *Nano Micro Lett.*, 14(2022), No. 1, p. 1.
- [11] H.G. Qin, L.L. Chen, L.M. Wang, X. Chen, and Z.H. Yang, V₂O₅ hollow spheres as high rate and long life cathode for aqueous rechargeable zinc ion batteries, *Electrochim. Acta*, 306(2019), p. 307.
- [12] M.Y. Yan, P. He, Y. Chen, et al., Water-lubricated intercalation in V₂O₅·nH₂O for high-capacity and high-rate aqueous rechargeable zinc batteries, *Adv. Mater.*, 30(2018), No. 1, art. No. 1703725.
- [13] N. Zhang, X.Y. Chen, M. Yu, Z.Q. Niu, F.Y. Cheng, and J. Chen, Materials chemistry for rechargeable zinc-ion batteries, *Chem. Soc. Rev.*, 49(2020), No. 13, p. 4203.
- [14] K.Y. Zhu, T. Wu, and K. Huang, NaCa_{0.6}V₆O₁₆·3H₂O as an ultra-stable cathode for Zn-ion batteries: The roles of pre-inserted dual-cations and structural water in V₃O₈ layer, *Adv. Energy Mater.*, 9(2019), No. 38, art. No. 1901968.
- [15] L. Cheng, J.W. Chen, Y. Yan, et al., Metal organic frameworks derived active functional groups decorated manganese monoxide for aqueous zinc ion battery, *Chem. Phys. Lett.*, 778(2021), art. No. 138772.
- [16] S.Y. Li, D.X. Yu, L.N. Liu, et al., In-situ electrochemical induced artificial solid electrolyte interphase for MnO@C nanocomposite enabling long-lived aqueous zinc-ion batteries, *Chem. Eng. J.*, 430(2022), art. No. 132673.
- [17] W.J. Li, X. Gao, Z.Y. Chen, et al., Electrochemically activated MnO cathodes for high performance aqueous zinc-ion battery, *Chem. Eng. J.*, 402(2020), art. No. 125509.
- [18] T.S. Zhang, Y. Tang, G.Z. Fang, et al., Electrochemical activation of manganese-based cathode in aqueous zinc-ion electrolyte, *Adv. Funct. Mater.*, 30(2020), No. 30, art. No. 2002711.
- [19] X.H. Chen, P.C. Ruan, X.W. Wu, S.Q. Liang, and J.A. Zhou, Crystal structures, reaction mechanisms, and optimization strategies of MnO₂ cathode for aqueous rechargeable zinc batteries, *Acta Phys. Chim. Sin.*, 38(2022), No. 12, art. No. 2111003.
- [20] D. Selvakumaran, A.Q. Pan, S.Q. Liang, and G.Z. Cao, A review on recent developments and challenges of cathode materials for rechargeable aqueous Zn-ion batteries, *J. Mater. Chem. A*, 7(2019), No. 31, p. 18209.
- [21] G. Zampardi and F. La Mantia, Prussian blue analogues as aqueous Zn-ion batteries electrodes: Current challenges and future perspectives, *Curr. Opin. Electrochem.*, 21(2020), p. 84.
- [22] Y.X. Zeng, X.F. Lu, S.L. Zhang, D.Y. Luan, S. Li, and X.W. Lou, Construction of Co–Mn Prussian blue analog hollow spheres for efficient aqueous Zn-ion batteries, *Angew. Chem. Int. Ed.*, 60(2021), No. 41, p. 22189.
- [23] L.N. Chen, Q.Y. An, and L.Q. Mai, Recent advances and prospects of cathode materials for rechargeable aqueous zinc-ion batteries, *Adv. Mater. Interfaces*, 6(2019), No. 17, art. No. 1900387.
- [24] Y.F. Geng, L. Pan, Z.Y. Peng, et al., Electrolyte additive engineering for aqueous Zn ion batteries, *Energy Storage Mater.*, 51(2022), p. 733.
- [25] B. Li, X.T. Zhang, T.T. Wang, et al., Interfacial engineering

- strategy for high-performance Zn metal anodes, *Nano Micro Lett.*, 14(2021), No. 1, p. 1.
- [26] T.T. Wang, C.P. Li, X.S. Xie, *et al.*, Anode materials for aqueous zinc ion batteries: Mechanisms, properties, and perspectives, *ACS Nano*, 14(2020), No. 12, p. 16321.
- [27] Q. Zhang, J.Y. Luan, Y.G. Tang, X.B. Ji, and H.Y. Wang, Interfacial design of dendrite-free zinc anodes for aqueous zinc-ion batteries, *Angew. Chem. Int. Ed.*, 59(2020), No. 32, p. 13180.
- [28] H.M. Yu, Y.J. Chen, H. Wang, *et al.*, Engineering multi-functionalized molecular skeleton layer for dendrite-free and durable zinc batteries, *Nano Energy*, 99(2022), art. No. 107426.
- [29] L. Hong, X.M. Wu, L.Y. Wang, *et al.*, Highly reversible zinc anode enabled by a cation-exchange coating with Zn-ion selective channels, *ACS Nano*, 16(2022), No. 4, p. 6906.
- [30] W.C. Du, E.H. Ang, Y. Yang, Y.F. Zhang, M.H. Ye, and C.C. Li, Challenges in the material and structural design of zinc anode towards high-performance aqueous zinc-ion batteries, *Energy Environ. Sci.*, 13(2020), No. 10, p. 3330.
- [31] N. Guo, W.J. Huo, X.Y. Dong, *et al.*, A review on 3D zinc anodes for zinc ion batteries, *Small Methods*, 6(2022), No. 9, art. No. e2200597.
- [32] R.T. Li, Y.X. Du, Y.H. Li, *et al.*, Alloying strategy for high-performance zinc metal anodes, *ACS Energy Lett.*, 8(2023), No. 1, p. 457.
- [33] B.T. Liu, S.J. Wang, Z.L. Wang, H. Lei, Z.T. Chen, and W.J. Mai, Novel 3D nanoporous Zn-Cu alloy as long-life anode toward high-voltage double electrolyte aqueous zinc-ion batteries, *Small*, 16(2020), No. 22, art. No. e2001323.
- [34] C. Liu, Z. Luo, W.T. Deng, *et al.*, Liquid alloy interlayer for aqueous zinc-ion battery, *ACS Energy Lett.*, 6(2021), No. 2, p. 675.
- [35] Q. Zhang, J.Y. Luan, L. Fu, *et al.*, The three-dimensional dendrite-free zinc anode on a copper mesh with a zinc-oriented polyacrylamide electrolyte additive, *Angew. Chem. Int. Ed.*, 58(2019), No. 44, p. 15841.
- [36] Y.M. Zhang, J.D. Howe, S. Ben-Yoseph, Y.T. Wu, and N. Liu, Unveiling the origin of alloy-seeded and nondendritic growth of Zn for rechargeable aqueous Zn batteries, *ACS Energy Lett.*, 6(2021), No. 2, p. 404.
- [37] P. Sun, L. Ma, W.H. Zhou, *et al.*, Simultaneous regulation on solvation shell and electrode interface for dendrite-free Zn ion batteries achieved by a low-cost glucose additive, *Angew. Chem. Int. Ed.*, 60(2021), No. 33, p. 18247.
- [38] H.J. Ji, Z.Q. Han, Y.H. Lin, *et al.*, Stabilizing zinc anode for high-performance aqueous zinc ion batteries via employing a novel inositol additive, *J. Alloys Compd.*, 914(2022), art. No. 165231.
- [39] C.P. Li, X.S. Xie, H. Liu, *et al.*, Integrated 'all-in-one' strategy to stabilize zinc anodes for high-performance zinc-ion batteries, *Natl. Sci. Rev.*, 9(2021), No. 3, art. No. nwab177.
- [40] Z.Y. Xing, S. Wang, A.P. Yu, and Z.W. Chen, Aqueous intercalation-type electrode materials for grid-level energy storage: Beyond the limits of lithium and sodium, *Nano Energy*, 50(2018), p. 229.
- [41] W. Kaveevivitchai and A. Manthiram, High-capacity zinc-ion storage in an open-tunnel oxide for aqueous and nonaqueous Zn-ion batteries, *J. Mater. Chem. A*, 4(2016), No. 48, p. 18737.
- [42] M.S. Chae, J.W. Heo, S.C. Lim, and S.T. Hong, Electrochemical zinc-ion intercalation properties and crystal structures of ZnMo₆S₈ and Zn₂Mo₆S₈ chevrel phases in aqueous electrolytes, *Inorg. Chem.*, 55(2016), No. 7, p. 3294.
- [43] W. Li, K.L. Wang, S.J. Cheng, and K. Jiang, An ultrastable presodiated titanium disulfide anode for aqueous "rocking-chair" zinc ion battery, *Adv. Energy Mater.*, 9(2019), No. 27, art. No. 1900993.
- [44] L.J. Yan, X.M. Zeng, Z.H. Li, *et al.*, An innovation: Dendrite free quinone paired with ZnMn₂O₄ for zinc ion storage, *Mater. Today Energy*, 13(2019), p. 323.
- [45] Y. Yang, J.F. Xiao, J.Y. Cai, *et al.*, Mixed-valence copper selenide as an anode for ultralong lifespan rocking-chair Zn-ion batteries: An insight into its intercalation/extraction kinetics and charge storage mechanism, *Adv. Funct. Mater.*, 31(2021), No. 3, art. No. 2005092.
- [46] W. Li, Y.S. Ma, P. Li, X.Y. Jing, K. Jiang, and D.H. Wang, Electrochemically activated Cu_{2-x}Te as an ultraflat discharge plateau, low reaction potential, and stable anode material for aqueous Zn-ion half and full batteries, *Adv. Energy Mater.*, 11(2021), No. 42, art. No. 2102607.
- [47] J. Cao, D.D. Zhang, Y.L. Yue, *et al.*, Strongly coupled tungsten oxide/carbide heterogeneous hybrid for ultrastable aqueous rocking-chair zinc-ion batteries, *Chem. Eng. J.*, 426(2021), art. No. 131893.
- [48] B. Wang, J.P. Yan, Y.F. Zhang, M.H. Ye, Y. Yang, and C.C. Li, *In situ* carbon insertion in laminated molybdenum dioxide by interlayer engineering toward ultrastable "rocking-chair" zinc-ion batteries, *Adv. Funct. Mater.*, 31(2021), No. 30, art. No. 2102827.
- [49] Q. Zhang, T.F. Duan, M.J. Xiao, *et al.*, BiOI nanopaper As a high-capacity, long-life and insertion-type anode for a flexible quasi-solid-state Zn-ion battery, *ACS Appl. Mater. Interfaces*, 14(2022), No. 22, p. 25516.
- [50] X. Wang, Y.M. Wang, Y.P. Jiang, *et al.*, Tailoring ultrahigh energy density and stable dendrite-free flexible anode with Ti₃C₂T_x MXene nanosheets and hydrated ammonium vanadate nanobelts for aqueous rocking-chair zinc ion batteries, *Adv. Funct. Mater.*, 31(2021), No. 35, art. No. 2103210.
- [51] T. Xiong, Y.X. Zhang, Y.M. Wang, W.S.V. Lee, and J.M. Xue, Hexagonal MoO₃ as a zinc intercalation anode towards zinc metal-free zinc-ion batteries, *J. Mater. Chem. A*, 8(2020), No. 18, p. 9006.
- [52] Y.P. Zhu, Y. Cui, and H.N. Alshareef, An anode-free Zn-MnO₂ battery, *Nano Lett.*, 21(2021), No. 3, p. 1446.
- [53] Y.Q. Jiang, K. Ma, M.L. Sun, Y.Y. Li, and J.P. Liu, All-climate stretchable dendrite-free Zn-ion hybrid supercapacitors enabled by hydrogel electrolyte engineering, *Energy Environ. Mater.*, 6(2023), No. 2, art. No. e12357.
- [54] K. Mao, J.J. Shi, Q.X. Zhang, Y. *et al.*, High-capacitance MXene anode based on Zn-ion pre-intercalation strategy for degradable micro Zn-ion hybrid supercapacitors, *Nano Energy*, 103(2022), art. No. 107791.
- [55] J.N. Hao, X.L. Li, X.H. Zeng, D. Li, J.F. Mao, and Z.P. Guo, Deeply understanding the Zn anode behaviour and corresponding improvement strategies in different aqueous Zn-based batteries, *Energy Environ. Sci.*, 13(2020), No. 11, p. 3917.
- [56] H. Jia, Z.Q. Wang, B. Tawiah, *et al.*, Recent advances in zinc anodes for high-performance aqueous Zn-ion batteries, *Nano Energy*, 70(2020), art. No. 104523.
- [57] W.J. Lu, C.X. Xie, H.M. Zhang, and X.F. Li, Inhibition of zinc dendrite growth in zinc-based batteries, *ChemSusChem*, 11(2018), No. 23, p. 3996.
- [58] C.P. Li, X.S. Xie, S.Q. Liang, and J. Zhou, Issues and future perspective on zinc metal anode for rechargeable aqueous zinc-ion batteries, *Energy Environ. Mater.*, 3(2020), No. 2, p. 146.
- [59] Z.Y. Xing, Y.Y. Sun, X.S. Xie, *et al.*, Zincophilic electrode interphase with appended proton reservoir ability stabilizes Zn metal anodes, *Angew. Chem. Int. Ed.*, 62(2023), No. 5, art. No. e202215324.
- [60] X.F. Chen, R.S. Huang, M.Y. Ding, H.B. He, F. Wang, and S.B. Yin, Hexagonal WO₃/3D porous graphene as a novel zinc intercalation anode for aqueous zinc-ion batteries, *ACS Appl. Mater. Interfaces*, 14(2022), No. 3, p. 3961.
- [61] B.B. Yang, T. Qin, Y.Y. Du, *et al.*, Rocking-chair proton battery based on a low-cost "water in salt" electrolyte, *Chem. Commun.*, 58(2022), No. 10, p. 1550.

- [62] Y.W. Cheng, L.L. Luo, L. Zhong, *et al.*, Highly reversible zinc-ion intercalation into chevrel phase Mo₆S₈ nanocubes and applications for advanced zinc-ion batteries, *ACS Appl. Mater. Interfaces*, 8(2016), No. 22, p. 13673.
- [63] M.S. Chae and S.T. Hong, Prototype system of rocking-chair Zn-ion battery adopting zinc chevrel phase anode and rhombohedral zinc hexacyanoferrate cathode, *Batteries*, 5(2019), No. 1, art. No. 3.
- [64] Z. Lv, B. Wang, M. Ye, Y. Zhang, Y. Yang, and C.C. Li, Activating the stepwise intercalation–conversion reaction of layered copper sulfide toward extremely high capacity zinc-metal-free anodes for rocking-chair zinc-ion batteries, *ACS Appl. Mater. Interfaces*, 14(2022), No. 1, p. 1126.
- [65] L. Wen, Y.N. Wu, S.L. Wang, *et al.*, A novel TiSe₂ (de)intercalation type anode for aqueous zinc-based energy storage, *Nano Energy*, 93(2022), art. No. 106896.
- [66] Y.Q. Du, B.Y. Zhang, R.K. Kang, *et al.*, Practical conversion-type titanium telluride anodes for high-capacity long-lifespan rechargeable aqueous zinc batteries, *J. Mater. Chem. A*, 10(2022), No. 32, p. 16976.
- [67] B.T. Zhao, S.L. Wang, Q.T. Yu, *et al.*, A flexible, heat-resistant and self-healable “rocking-chair” zinc ion microbattery based on MXene-TiS₂ (de)intercalation anode, *J. Power Sources*, 504(2021), art. No. 230076.
- [68] N.N. Liu, X. Wu, Y. Zhang, *et al.*, Building high rate capability and ultrastable dendrite-free organic anode for rechargeable aqueous zinc batteries, *Adv. Sci.*, 7(2020), No. 14, art. No. 2000146.
- [69] Y. Liu, X.M. Zhou, X. Wang, *et al.*, Hydrated titanate as an ultralow-potential anode for aqueous zinc-ion full batteries, *Chem. Eng. J.*, 420(2021), art. No. 129629.
- [70] S.L. Leng, X.Y. Sun, Y.C. Yang, and R.H. Zhang, Borophene as an anode material for Zn-ion batteries: A first-principles investigation, *Mater. Res. Express*, 6(2019), No. 8, art. No. 085504.